P. M. Marcus
F. P. Jona
D. W. Jepsen

Energy Diagram Method for Bragg Reflections in Low Energy Electron Diffraction (LEED) Spectra

Abstract: A point of view and a method of calculation derived from energy band theory are applied to the problem of finding energies of Bragg reflections from a given crystal. Energy curves are defined and calculated which describe the behavior of individual diffracted electron beams for a given set of beams incident on a particular face of the crystal. Intersections of these curves correspond to and identify the Bragg reflections associated with each beam. Energy diagrams and Bragg peak positions are shown for simple cubic and face-centered cubic lattices for various angles of incidence. We discuss the method in some simple cases and then solve the problem of finding Bragg reflections from the general crystal lattice with an arbitrary surface plane and arbitrary incident beams. The effect of the surface in producing well-defined diffracted beams for any incident beam and in grouping the Bragg reflections into these beams is described. Tables and formulas, which apply to any direction of incidence, are given for the Bragg reflections from the (001), (110) and (111) faces of the face-centered cubic lattice.

Introduction

Low energy electron diffraction (LEED) spectra are a record of the intensity distribution of electrons diffracted by a crystal surface in terms of three parameters, the energy and two angles, which define the incident electron beam. The diffracted electrons emerge from the crystal in a finite number of discrete beams that can be recorded individually. Figure 1 shows a typical curve of the variation with energy for constant angle of incidence of one diffracted beam, the 00 or specularly reflected beam from a (001) surface of aluminum. The observed spectra yield information about the electronic state of the crystal, provided that the difficult problem of calculating the scattering can be solved. One limiting case can, in fact, be completely solved and that is the case of a vanishingly weak crystal potential. In this case the problem reduces to the calculation of Bragg reflections. Long ago the problem was expressed as an explicit set of algebraic relations embodied in the Laue or Bragg interference conditions and was solved by the Ewald construction. The solution in this limiting case is a useful guide to the solution of the problem in which there is a finite potential.

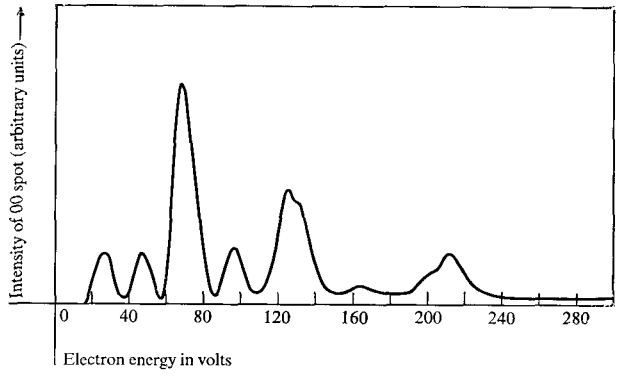

Figure 1 Experimental energy dependence of the intensity of the specularly reflected (or 00) beam from a {001} surface of Al at nearly normal incidence. (The spectrum has not been corrected to constant incident-electron current.)

The object of this paper is to present an alternative method of solution of the Bragg reflection problem, which we call the energy diagram method and which is closely related to the formulation of energy band problems. In addition to providing a practical solution with certain advantages over the Ewald method, the energy diagram method is directly related to a particular crystal surface and provides an immediate way of assigning each Bragg reflection to a diffracted beam. Thus it gives useful insight into the meaning of a diffracted beam and permits calculation of the direction of such beams for any beam

P. M. Marcus and D. W. Jepsen are located at the IBM Thomas J. Watson Research Center, Yorktown Heights, New York 10598; F. P. Jona's current address is Department of Materials Science, State University of New York at Stony Brook, Stony Brook, New York 11790.

incident on a given crystal surface. These directions are also part of Bragg reflection theory and do not depend on the strength of the potential.

For initial information and later reference, it is useful to state the interference conditions now and to compare in general terms the Ewald and energy diagram methods of satisfying them. The Laue or Bragg interference conditions, which determine the scattered plane waves of wave vector $\mathbf{k}^s$, produced by the effect of the crystal potential on the incident plane wave of wave vector $\mathbf{k}^i$, can be written as a vector and a scalar equation:

$$\mathbf{k}^s = \mathbf{k}^i + n_1\mathbf{b}_1 + n_2\mathbf{b}_2 + n_3\mathbf{b}_3 \tag{1}$$

and

$$\epsilon^i = (\mathbf{k}^i)^2 = \epsilon^s = (\mathbf{k}^s)^2. \tag{2}$$

The $\mathbf{b}_1$, $\mathbf{b}_2$, $\mathbf{b}_3$ vectors are reciprocal-lattice basis vectors and n_1, n_2, n_3 are integers. Equation (2) expresses the condition of elastic scattering, so that the energies ϵ^i and ϵ^s of the waves are equal, as are the magnitudes of $\mathbf{k}^i$ and $\mathbf{k}^s$†.

In the Ewald construction the energy condition is the first condition satisfied. One forms a spherical surface in three-dimensional reciprocal space with radius k^i and an appropriate center and then one satisfies the three conditions of the vector relation (1) by finding points of the reciprocal lattice that lie on the surface of the sphere. In the energy diagram method a set of curves in two dimensions is constructed first. These curves automatically satisfy two of the three vector relations in (1); the other two conditions (on the third components of $\mathbf{k}^s$ and $\mathbf{k}^i$ and on ϵ^s and ϵ^i) are then satisfied by finding intersections of these curves with each other. Because all the required curves can be drawn on a two-dimensional graph, this method is constructionally simpler than the Ewald method. In addition, the energy diagram method immediately leads to the idea of diffracted beams and to the Bragg reflections associated with each beam‡ because there is a particular curve for each beam and the associated Bragg reflections correspond to the intersections of that curve with other curves.

The energy diagram method is developed in three stages of increasing complexity. First, the basic idea is applied to the simple case of normal incidence on the (001) face of a cubic crystal. This case permits natural introduction of the energy curve for each beam and also the replotting of these curves vs. reduced wave vector. The various Bragg reflections associated with each beam are then indicated. Second, the problem is generalized in two ways: We consider a more general class of lattices and surfaces (although these satisfy a special orthogonality condition) and we remove the restrictions imposed on the set of incident beams. (This latter generalization, however, complicates the definition of the individual beam curves.) Third, we describe the application of this method to cases in which beams with fixed orientation but with continuously increasing energy are incident on the (001) surfaces of simple cubic (sc) and face-centered cubic (fcc) lattices. The dependence of the Bragg reflections on the polar and azimuthal angles of the incident beam is shown directly.

Finally, the general problem of Bragg scattering by a crystal lattice with an arbitrary surface plane is solved. Now, for the first time, the surface is not built into the coordinate system used and the complete set of Bragg reflections is discussed without reference to a surface. The general theory of the transformation of the indices of a Bragg reflection between sets of basis vectors is given, the effect of the surface in producing well-defined scattered beams for all incident beams is analyzed and a procedure is given for assigning all Bragg reflections to the appropriate beam (which requires a suitable set of basis vectors). This assignment procedure is demonstrated for various surfaces of the fcc lattice and we include a table which describes by their cubic components, i.e., by their components along the usual cubic axes of the fcc lattice, the Bragg reflections in ten beams from the (001), (110) and (111) surfaces. The energies at which the Bragg reflection peaks appear in the LEED spectra for any incident beam direction can be calculated readily from these components. The generalization of the energy diagram method to the case of a general lattice and surface and an arbitrary incident beam is described in detail.

The complete set of Bragg reflections in each beam, corresponding to the complete set of intersections of that energy curve with other energy curves, implicitly indicates all possible peaks in the LEED spectra of the various beams (with one interesting exception). This paper does not include a discussion of the detailed correspondence of the Bragg reflections to the possible peaks, but we note that the peaks can be classified as primary, secondary and tertiary. The primary peaks are understood readily as the result of a single Bragg reflection; explanation of the other classes of peaks can be made with a simple multiple scattering rule for plane waves in a crystal with a specified surface. In the rule the concept of "incomplete Bragg reflection" is introduced and used in a chain of reflections. Thus knowledge of the positions of Bragg reflections makes evident the maximum possible number of LEED peaks and allows one to estimate the peak energies; however, the solution of the general (dynamic) scattering problem with a finite crystal potential[1,2] must be available before one can estimate the LEED intensities and actual positions of any of these peaks.

† It is convenient to use the units of band theory in which energy is expressed in rydbergs and distance in Bohr radii; thus the energy of a plane wave $\exp(i\mathbf{k}\cdot\mathbf{r})$ is $\epsilon = k^2$.

‡ The Bragg reflections are also described as being "assigned to" or "in" a beam.

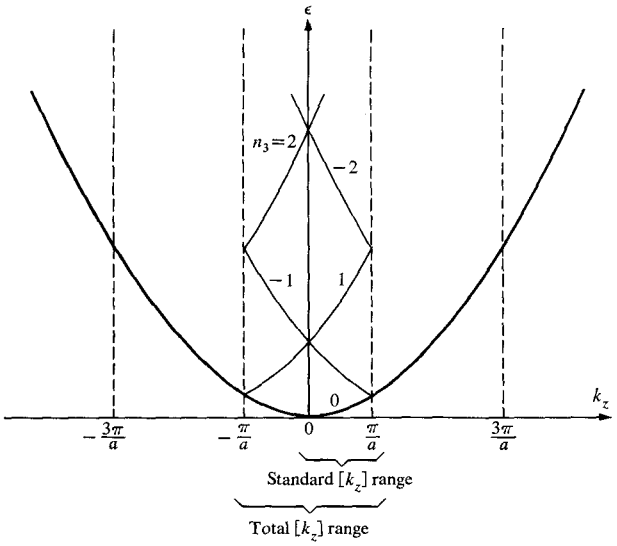

Figure 2 Energy ϵ of a beam incident normal to the (001) surface of a simple cubic lattice as a function of the normal component k_z of the wave vector.

Bragg reflections of a normally incident beam

The energy diagram method of locating Bragg reflections is conveniently illustrated by the simple case in which a beam is incident normally on the (001) face of a cubic lattice. For this case $\mathbf{k}^i = (0, 0, k_z^i)$, where the z axis is normal to the surface. The first graphic curve used represents the energy of the incident beam as a function of k_z, i.e., $\epsilon(k_z) = k_z^2$; this is shown in Fig. 2. The basic curve of the energy diagram method is then obtained by plotting ϵ vs. $[k_z]$, the reduced value of k_z.† Here we use the symbol $[k_z]$ to denote the residual value of k_z in the range $-\pi/a$ to $+\pi/a$ after integral multiples of $2\pi/a$, the magnitude of the shortest reciprocal-lattice vector in the z direction, have been subtracted from k_z; i.e.,

$$[k_z] = k_z \bmod (2\pi/a) = k_z - 2\pi n_3/a. \tag{3}$$

Similar definitions apply to $[k_x]$ and $[k_y]$. The plot of ϵ vs. $[k_z]$ converts the continuous curve $\epsilon(k_z)$ into a characteristic ladder-like structure over the range $-\pi/a \leqq [k_z] \leqq \pi/a$. Each branch of the curve has an index n_3; i.e., the function $\epsilon(k_z)$ for $-\infty \leqq k_z \leqq \infty$ is equivalent to the set of functions $\epsilon_{n_3}([k_z])$ for $n_3 = 0, \pm1, \pm2, \cdots$ and $-\pi/a \leqq [k_z] \leqq \pi/a$, as shown in Fig. 2. If we make use of the symmetry in k_z of the energy curve, $\epsilon(k_z) = \epsilon(-k_z)$, which exists in our applications (although more general cases can occur), the entire energy curve is completely described in the standard range $0 \leqq [k_z] \leqq \pi/a$ used in succeeding diagrams.

† The concepts of reduced wave vector, reduced Brillouin zone and free-electron energy diagram are well known and fundamental in solid-state theory. For further definitions, discussion and illustrations see, for example, Ziman[3] (p. 20 *et seq.*) and Slater[4] (p. 250 *et seq.*).

At the intersections of the successive branches of the reduced curve, which occur at the edges $[k_z] = 0$ and π/a of the standard range, the wave vectors on the two branches have the same values of ϵ and $[k_z]$; also $[k_x] = [k_y] = 0$ for normal incidence. Thus the Laue conditions are all satisfied if one of these wave vectors is $\mathbf{k}^i$ and the other is $\mathbf{k}^s$. Because only k_z changes (from positive for the incident wave, assumed to be traveling toward increasing values of z, to negative for the scattered wave), this particular intersection represents a principal Bragg peak corresponding to specular reflection of the normally incident electron beam into the 00 reflected beam.

We now introduce a new set of energy curves $\epsilon_{n_1 n_2}(k_z)$, $n_1, n_2 = 0, \pm1, \pm2, \cdots$, which are obtained by adding reciprocal-lattice vectors in the surface plane to $\mathbf{k}^i$; i.e.,

$$\epsilon_{n_1 n_2}(k_z) = (2\pi n_1/a)^2 + (2\pi n_2/a)^2 + k_z^2.$$

When $\epsilon_{n_1 n_2}$ is plotted vs. $[k_z]$, a set of branches in the standard range is obtained which can be labeled $\epsilon_{n_1 n_2 n_3}([k_z])$. At each intersection of two branches the Laue conditions are again satisfied for any n_1, n_2, n_3 because $[k_x] = [k_y] = 0$ for all curves in the diagram. The intersection of $\epsilon_{n_3} (\equiv \epsilon_{00n_3})$ with any other branch $\epsilon_{n_1 n_2 n_3}$ (n_1, n_2 not both zero) corresponds to a Bragg reflection in which k_x and k_y change; hence the scattered wave is not the 00 beam. A primary Bragg peak is expected in the $n_1 n_2$ beam at this energy and the dynamical theory shows that appreciable intensity can also occur in the 00 beam, thus constituting a secondary peak.‡

Generalized free-electron energy curves and the location of Bragg reflections

Consider a semi-infinite crystal with periodicity in the plane parallel to the surface specified by basic reciprocal-lattice vectors

$$\mathbf{b}_1 = b_{11}\hat{\imath}_x + b_{12}\hat{\imath}_y \quad \text{and} \quad \mathbf{b}_2 = b_{21}\hat{\imath}_x + b_{22}\hat{\imath}_y, \tag{4}$$

where $\hat{\imath}_x$ and $\hat{\imath}_y$ are unit vectors along rectangular axes in the plane (Fig. 3); $\mathbf{b}_1$ and $\mathbf{b}_2$ need not be primitive vectors, although the discussion is simpler when they are primitive. We treat a special class of orthogonal lattices in which the surface plane contains two of the reciprocal lattice vectors, $\mathbf{b}_1$ and $\mathbf{b}_2$, while the third, $\mathbf{b}_3$, is perpendicular to the surface. Again $\mathbf{b}_3$ need not be primitive, but use of the primitive vector simplifies the problem.

The set of incident beams is now generalized to any continuous variation of the energy and orientation parameters determining $\mathbf{k}^i$. We can think of following a curve in $\mathbf{k}$

‡ A more detailed discussion of the correspondence of intersections of energy curves with the various kinds of Bragg peaks is given in the next section.

space (which differs from reciprocal-lattice space by the factor 2π) specified by parametric equations of the form $k_x^i = k_x(t)$, $k_y^i = k_y(t)$ and $k_z^i = k_z(t)$. Note that the energy is also a function of the parameter t (for simplicity this function will be assumed to be monotonic),

$$\epsilon(t) = k_x(t)^2 + k_y(t)^2 + k_z(t)^2, \tag{5}$$

and can be plotted vs. $k_z(t)$ to obtain the curve $\epsilon(k_z)$ indicated in Fig. 2. However, the basic plot used to locate diffraction peaks is the curve of ϵ vs. $[k_z]$, the residual value when integral multiples of b_3 are subtracted from k_z to obtain a reduced value in the range $-\frac{1}{2}b_3 \leqq [k_z] \leqq \frac{1}{2}b_3$. If the symmetric energy curve at $-k_z$ is also reduced in this way, the complete ϵ curve is given by a series of branches in the smaller standard range $0 \leqq [k_z] \leqq \frac{1}{2}b_3$. Each branch has an index n_3 such that

$$k_z = [k_z] + n_3 b_3. \tag{6}$$

Now we construct from $\epsilon(k_z)$ a discrete set of curves $\epsilon_{n_1 n_2}(k_z)$ corresponding to the integral indices n_1, $n_2 = 0, \pm 1, \pm 2, \cdots$. These are obtained by plotting $\epsilon(t)$ against a function $k_z^s(t)$ defined by

$$[k_x(t)\hat{\imath}_x + k_y(t)\hat{\imath}_y + n_1\mathbf{b}_1 + n_2\mathbf{b}_2]^2 + k_z^s(t)^2$$
$$= k_x(t)^2 + k_y(t)^2 + k_z(t)^2 = \epsilon(t). \tag{7}$$

Thus $k_z^s(t)$ is a new value of the z component of $\mathbf{k}(t)$ which preserves the energy $\epsilon(t)$ by compensating the addition of a reciprocal lattice vector in the x-y plane to the component of $\mathbf{k}$ parallel to the surface [in Eq. (7) this vector is $n_1\mathbf{b}_1 + n_2\mathbf{b}_2$]. The transformation from $\epsilon(k_z)$, which is also denoted by $\epsilon_{00}(k_z)$, to $\epsilon_{n_1 n_2}(k_z)$ is shown in Fig. 4. As n_1 and n_2 increase in magnitude, the minimum value of ϵ for which (7) has a solution for real k_z^s will increase, so that at a given ϵ only a finite number of curves $\epsilon_{n_1 n_2}$ exists.

If all the curves $\epsilon_{n_1 n_2}$ are now translated into the standard range of $[k_z]$ as in Fig. 2, so that each curve becomes a series of branches labeled by an n_3 value, all intersections of the various branches correspond to Bragg reflections and the true nonreduced $\mathbf{k}$ values on each pair of intersecting curves are related by the Laue conditions. This latter result follows directly from the construction of the $\epsilon_{n_1 n_2}$ curves which provides that, if two points on two $\epsilon_{n_1 n_2}$ curves have the same energy, the surface-plane components of their wave vectors differ by a reciprocal-lattice vector.† Because the occurrence of an intersection means

† In the preceding section, which treats the case of a normally incident electron beam, all points on the curves in the energy diagram have k_x and k_y values that differ by reciprocal-lattice vectors (i.e., $[k_x]$ and $[k_y]$ are the same and, in fact, are both zero for normal incidence). The more general case treated in this and the following section cannot be based on such a simple relation; one replaces it by making the k_x and k_y values for points with the same energy on different curves differ by reciprocal-lattice vectors. These transverse components vary in magnitude as we follow any one curve.

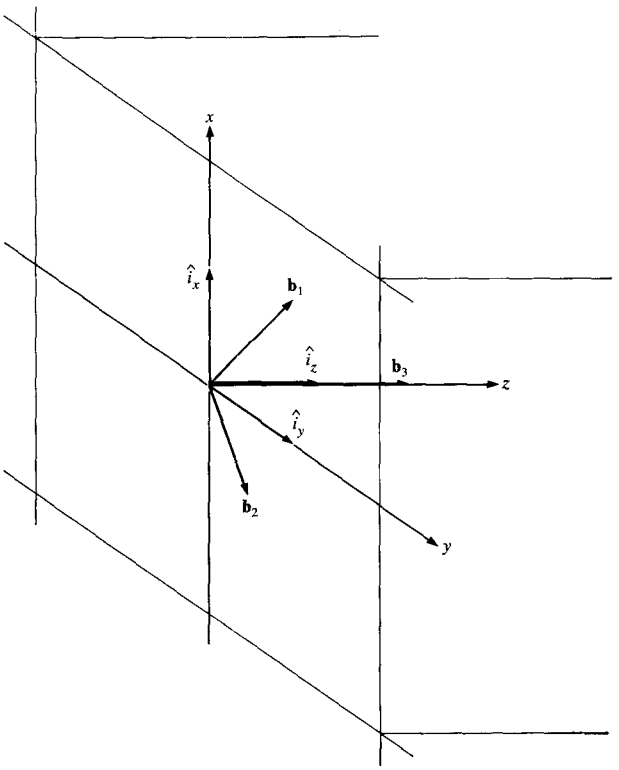

Figure 3 Geometry of the semi-infinite crystal showing the orthogonal unit vectors $\hat{\imath}_x$, $\hat{\imath}_y$, $\hat{\imath}_z$ and the basic reciprocal-lattice vectors $\mathbf{b}_1$, $\mathbf{b}_2$, $\mathbf{b}_3$; $\mathbf{b}_1$ and $\mathbf{b}_2$ are in the surface plane and $\mathbf{b}_3$ is perpendicular to the surface.

Figure 4 Construction of the curve $\epsilon_{n_1 n_2}(k_z)$ from the $\epsilon_{00}(k_z)$ curve [see Eq. (7) in the text].

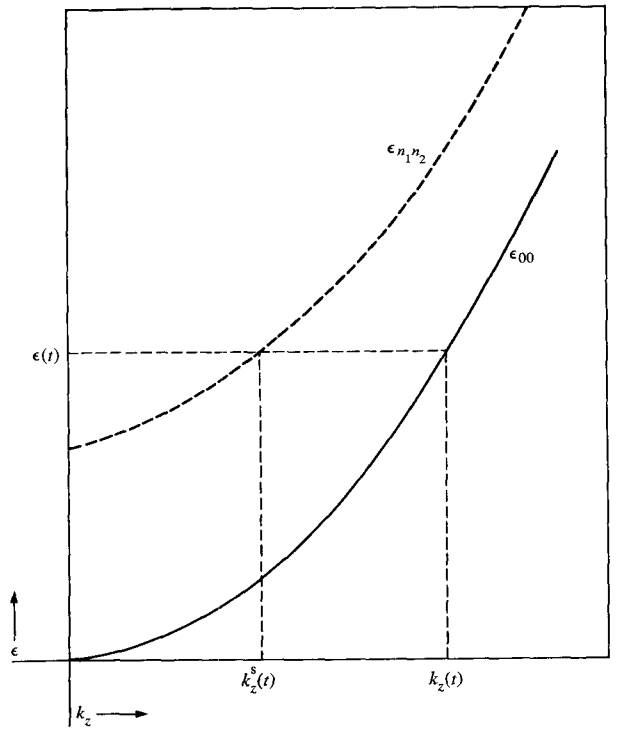

that the energies corresponding to points on two curves are equal and that the $[k_x]$ values of those points are also equal (the k_x values differ by a reciprocal-lattice vector), all the conditions contained in Eqs. (1) and (2) are satisfied.

We now indicate the relations between these intersections and the peaks in the beam intensities, but do not give a detailed discussion. The intersections of an energy curve $\epsilon_{n_1 n_2}$ in the reduced diagram are of two kinds: (1) intersections with ϵ_{00} and (2) intersections with $\epsilon_{m_1 m_2} \neq \epsilon_{00}$. Intersections of the first kind correspond to a primary peak in the $n_1 n_2$ beam and to secondary peaks in all other beams at the same energy (this includes the case $n_1 n_2 = 00$). Intersections of the second kind with $n_1 n_2 \neq 00$ correspond to secondary peaks in the $m_1 m_2$ and $n_1 n_2$ beams and to tertiary peaks in all other beams. As the crystal potential increases in strength, the peak positions shift, usually to lower energies because the average potential is negative. In general, primary peaks are stronger than secondaries, which are stronger than tertiaries; quantitative evaluation of intensities, positions and widths requires solution of the multiple scattering problem.

This exhaustive classification of peaks and their correspondence to the intersections in the energy diagram can be understood qualitatively from simple multiple scattering considerations.† The existence of secondary and tertiary peaks is explained by the following tentative rule (suggested by detailed calculation) for the occurrence of "incomplete Bragg reflections": Given a plane wave of energy ϵ propagating in the lattice, scattering will occur with strength dependent on the potential into plane waves which (1) have the same ϵ, (2) satisfy the Laue conditions on k_x and k_y but *not* on k_z and (3) have the same orientation in the lattice with respect to the surface (i.e., the same sign of k_z).‡ Thus scattering can occur into other waves without intersection of the corresponding energy curves; the curves need only have the same slope. The abandonment of the Laue condition on k_z corresponds to the loss of complete translational symmetry in the z direction due to the presence of the surface and is discussed in more detail later. Then, with this rule, it is easy to show that intensity in the various peaks can be built up by a chain of at most three reflections. One of these must be a complete Bragg reflection (requiring an intersection of two curves) which reverses the direction of the z component of the wave; the others are incomplete Bragg reflections (of the type defined above) in the forward or reverse directions, at most one in each direction. These latter reflections require the presence of other, nonintersecting, curves at the energy corresponding to the peak.§

A relation between the energies and the k_z values at which diffraction peaks appear can be obtained from Eq. (7) by setting $k_z^s = k_z + n_3^d b_3$ (n_3^d denotes the change in k_z in the diffraction process and is equal to the difference $n_3^s - n_3$, where $k_z^s = [k_z^s] + n_3^s b_3$); this procedure gives

$$2k_x(n_1 b_{11} + n_2 b_{21}) + 2k_y(n_1 b_{12} + n_2 b_{22}) + 2k_z n_3^d b_3$$
$$= -[(n_1 b_{11} + n_2 b_{21})^2 + (n_1 b_{12} + n_2 b_{22})^2 + (n_3^d b_3)^2]. \quad (8)$$

For given values of n_1, n_2 and n_3^d and for general functions $k_x(t)$, $k_y(t)$ and $k_z(t)$ defining the incident beam, Eq. (8) is an implicit equation for the values t_d at which diffraction takes place; from t_d the corresponding values of $\epsilon(t_d)$ and $k_z(t_d)$ can be determined.

For the special functional forms in the important case of a beam incident at a fixed orientation with respect to the surface, we have

$$\begin{aligned} k_x &= k \sin\theta \cos\phi, \\ k_y &= k \sin\theta \sin\phi, \\ k_z &= k \cos\theta \end{aligned} \quad (9)$$

and the parameter t is the amplitude $k = \epsilon^{\frac{1}{2}}$. Then we obtain from Eq. (8)

$$\begin{aligned} \epsilon^{\frac{1}{2}} = k &= -[(n_1 b_{11} + n_2 b_{21})^2 \\ &\quad + (n_1 b_{12} + n_2 b_{22})^2 + (n_3^d b_3)^2] \\ &\quad \div \{2[\sin\theta \cos\phi\,(n_1 b_{11} + n_2 b_{21})] \\ &\quad + 2[\sin\theta \sin\phi\,(n_1 b_{12} + n_2 b_{22}) \\ &\quad + \cos\theta\,(n_3^d b_3)]\}. \end{aligned} \quad (10)$$

This expression is simplified further in the cubic lattice applications for which $\mathbf{b}_1$ and $\mathbf{b}_2$ are parallel to the x and y axes.¶

Application to the simple and face-centered cubic lattices

The application of the energy diagram method to the (001) face of the simple cubic (sc) lattice is shown in Fig. 5a. This diagram differs from Fig. 2 in that a normalized energy scale ϵa^2 is used (applicable to sc lattices with any value of the cubic cell edge a) and the wave number is

† Watts[5] describes LEED intensities from the point of view of multiple scattering of plane waves and obtains the three kinds of peaks from his formalism.

‡ Some scattering occurs into waves with the opposite direction in the lattice, but this scattering appears to be weaker than that into the same direction; hence, for the qualitative purpose of locating peaks we ignore this additional scattering.

§ An exceptional case occurs when two intersecting reduced curves have slopes with the same sign. Then, as pointed out by Jennings and McRae,[6] no LEED peak is produced. This case can also be understood from our rule because this Bragg reflection does not reverse k_z and any incomplete Bragg reflection cannot reverse k_z. Hence no reflected wave can be produced because no step in the chain can reverse k_z.

¶ Equation (10) is equivalent to one given by Laue in the analysis of x-ray diffraction.[7]

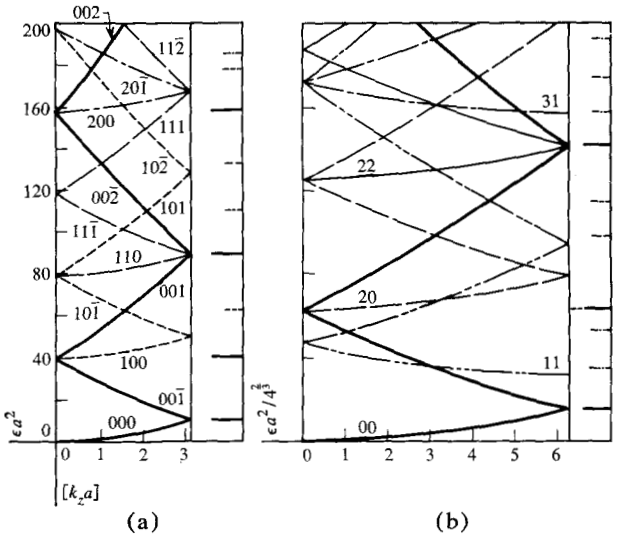

Figure 5 Free-electron energy diagrams for a beam incident normally ($\theta = \phi = 0$) on a (001) surface of (a) a simple cubic lattice and (b) a face-centered cubic lattice. The line spectrum on the right-hand side of each diagram is the possible 00 spectrum for the case considered. The ordinate unit is *rydberg-(Bohr radius)*^{2}.

reduced to a dimensionless scale $[k_z a]$ that is independent of a. In addition, the higher order bands $\epsilon_{n_1 n_2}([k_z a])$ with n_1 and n_2 different from zero have been introduced and the n_1, n_2, n_3 values have been used to label the branches of each band. For the case of normal incidence, the higher order bands are all degenerate; thus the 100 branch also refers to the 010, $\bar{1}00$ and $0\bar{1}0$ branches, etc. All intersections of the branches of the 00 band (drawn as solid lines) with each other or with branches of higher order bands (dashed lines) indicate the energies of the Bragg peaks (primary and secondary, respectively). The 00 Bragg reflection spectrum is shown at the right of the diagram (Fig. 5a); the reflections are drawn as horizontal lines, those corresponding to the primary peaks being longer and continuous. Not all lines will appear with appreciable strength in the actual spectrum (the detailed theory of scattering by the crystal potential is needed to determine the intensities), but the Bragg spectrum in Fig. 5 indicates which lines are possible. In general, the primary peaks corresponding to electrons scattered directly into the 00 beam are stronger than the secondaries.†

The diagram in Fig. 5b is a similar plot for normal incidence on the (001) face of a fcc lattice. The normalized energy scale includes a factor $4^{-\frac{2}{3}}$ to relate it to a crystal with the same atom density as the sc crystal (a is always the unit cell edge, not a primitive cell edge in the fcc case).

† To obtain the complete Bragg spectrum, the positions of the tertiary peaks should also appear on the right-hand side of Figs. 5a and 5b.

The energy diagram for normal incidence ($\theta = 0$) on the (001) face of the sc lattice is shown in Fig. 6a. Cases of oblique incidence are shown in Figs. 6b and 6c. In Fig. 6b $\theta = 6°$ and $\phi = 0$; some but not all of the degeneracy of the bands is removed; e.g., the 01 and $0\bar{1}$ bands and the $\bar{1}1$ and $\bar{1}\bar{1}$ bands are still degenerate (only the initial branch of each band is labeled). All of the degeneracies are removed in the example of Fig. 6c in which $\theta = 6°$ and $\phi = 26°34'$. The 00 Bragg spectrum on the right-hand side of each diagram shows an increasing number of secondary lines as the degeneracy is removed progressively.

Figure 7 is similar to Fig. 6, but applies to the (001) face of a fcc lattice. As in Fig. 5, the n_1, n_2 labels of the band are different from the sc case (only n_1, n_2, n_3 all even or all odd are allowed).

The angular dependence of the Bragg lines is shown for the fcc lattice in Figs. 8 and 9; here only the intersection points of the 00 branches of Fig. 7 are plotted as functions of angle. In Fig. 8 the θ dependence of primary peaks (solid lines) and secondary peaks (dashed lines) is shown for two values of ϕ; in Fig. 9 the ϕ dependence is shown for two values of θ. These curves are based on Eq. (10) specialized to the case $b_{11} = b_{22} = b_3 = 2\pi/a$, $b_{21} = b_{12} = 0$:

$$\epsilon^{\frac{1}{2}} a = \frac{-\pi(n_1^2 + n_2^2 + n_3^{d2})}{(n_1 \cos\phi + n_2 \sin\phi)\sin\theta + n_3^{d} \cos\theta}.$$

A vertical section of Fig. 8 or 9 gives the discrete Bragg spectrum as a function of energy at the particular angles selected by the section; a horizontal section, however, gives a Bragg spectrum as a function of one angle at given values of the energy and the other angle. The principal Bragg peaks are independent of ϕ and change slowly with θ for small values of θ. The secondary peaks, however, show stronger θ and ϕ dependence.

Bragg reflections for a general lattice

Bragg reflections in special simple situations, namely when two reciprocal-lattice basis vectors are in the surface plane and the third is perpendicular to the plane, were discussed in the preceding sections. This class includes many of the important practical cases and was used for easy introduction of the energy diagram for the beams of a particular surface and for identifying Bragg reflections by intersections of two energy curves or beam lines on the reduced plot. The reflections occurring in a particular beam can be determined by the intersections of that beam line with other beam lines. However, if more general cases are to be studied it is necessary to solve the problem of locating Bragg reflections for a general lattice and to assign those reflections to the various beams characteristic of an arbitrary surface plane. The solution includes the previous special cases, but requires more-formal development and notation. It is convenient to discuss

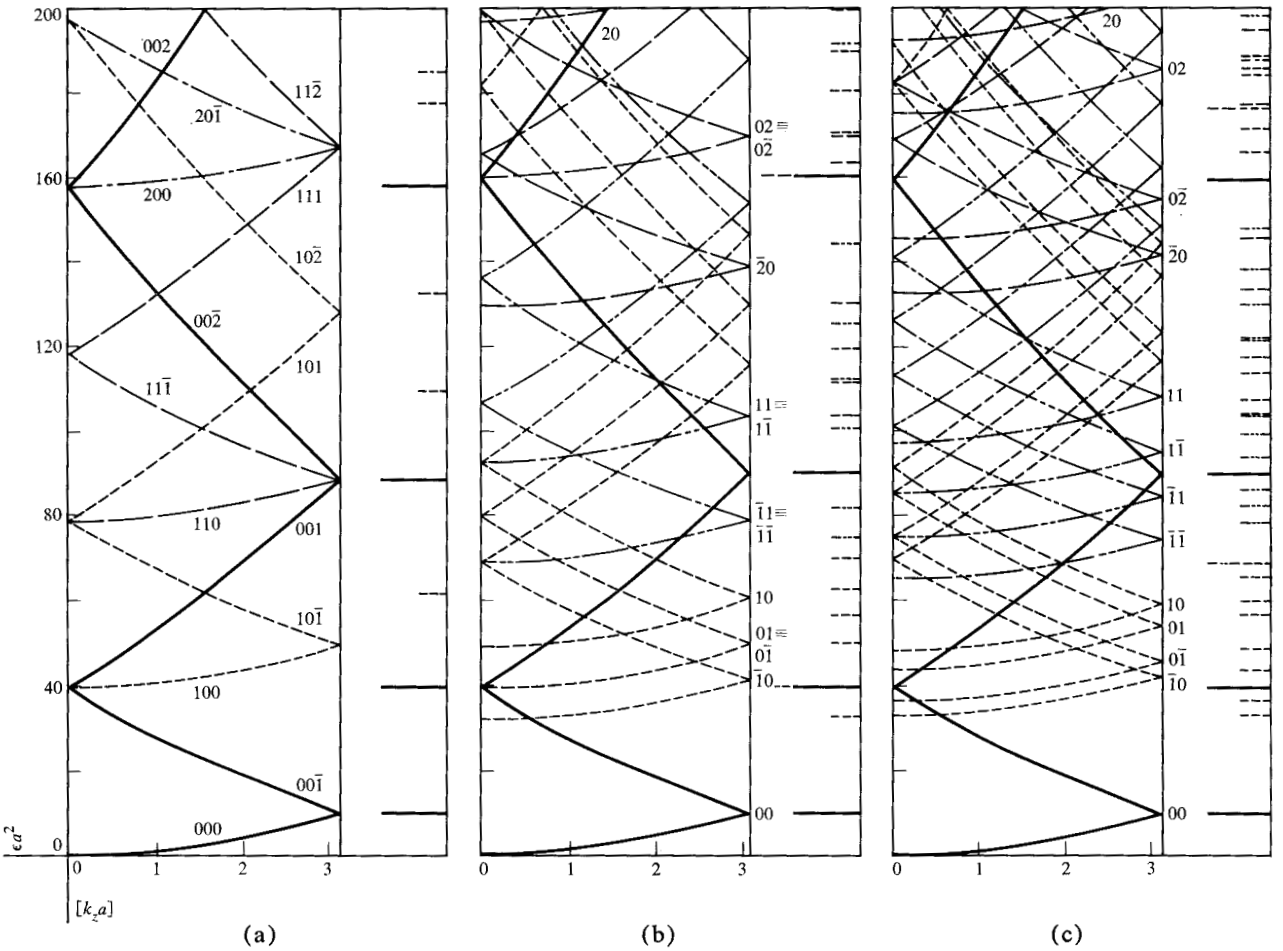

Figure 6 Free-electron energy diagrams for a beam incident with orientation (a) $\theta = \phi = 0$ (normal incidence); (b) $\theta = 6°$, $\phi = 0$; and (c) $\theta = 6°$, $\phi = 26°34'$ on a (001) surface of a simple cubic crystal. The ordinate unit is *rydberg-(Bohr radius)*^{2}.

first all the Bragg reflections of a crystal lattice for a given set of incident beams without reference to a surface and without assigning the reflections to beams. Then a surface is introduced, the definition of a beam is established and the Bragg reflections are classified according to the beam in which they occur on each surface. Finally, explicit application to various surfaces of the fcc lattice is described.

• *Integral indices and energies of all Bragg reflections*

Let the general lattice be described by a basis set of reciprocal lattice vectors $\mathbf{b}_j$, $j = 1, 2, 3$†; the discussion of Bragg reflections does not require the use of coordinate-space lattice vectors, which we introduce later. Consider a set of incident beams $\mathbf{k}^i(t)$, where t is a continuously varying parameter specifying a member of the set. The special case of a beam with fixed orientation but with nonconstant $|\mathbf{k}|$ or ϵ is of particular interest. In this case k (or $\epsilon = k^2$) serves as a parameter and we set

$$\mathbf{k}^i = k\hat{k}(\theta, \phi), \tag{11}$$

where $\hat{k}(\theta, \phi)$ is a unit vector oriented at angles θ and ϕ with respect to suitable axes fixed in the crystal lattice. The effect of the lattice on the incident wave is to scatter that wave into the set of scattered waves $\mathbf{k}^s$ obtained by adding a general reciprocal-lattice vector to $\mathbf{k}^i$,

$$\mathbf{k}^s = \mathbf{k}^i + (n_1\mathbf{b}_1 + n_2\mathbf{b}_2 + n_3\mathbf{b}_3) \equiv \mathbf{k}^i + \mathbf{n}. \tag{12}$$

The plane wave $\exp(i\mathbf{k}^s \cdot \mathbf{r})$ has the same translational symmetry as the plane wave $\exp(i\mathbf{k}^i \cdot \mathbf{r})$; the added terms $\mathbf{b}_j$ do not affect the phase factor of the wave when $\mathbf{r}$ changes by a lattice vector $\mathbf{R}$. However, the scattered wave does not have a strong amplitude unless the additional condition that the scattered and incident waves have the same energy (or $|\mathbf{k}^s| = |\mathbf{k}^i|$) is satisfied, in which case the wave is said to be Bragg-reflected. Thus the scattered

† The basis vectors $\mathbf{b}_j$ include a factor of 2π in their definition as shown in Eqs. (19) and (20). This inclusion is customary in band theory because the $\mathbf{b}_j$ form the basis for k space, which is related to reciprocal-lattice space by a factor of 2π.

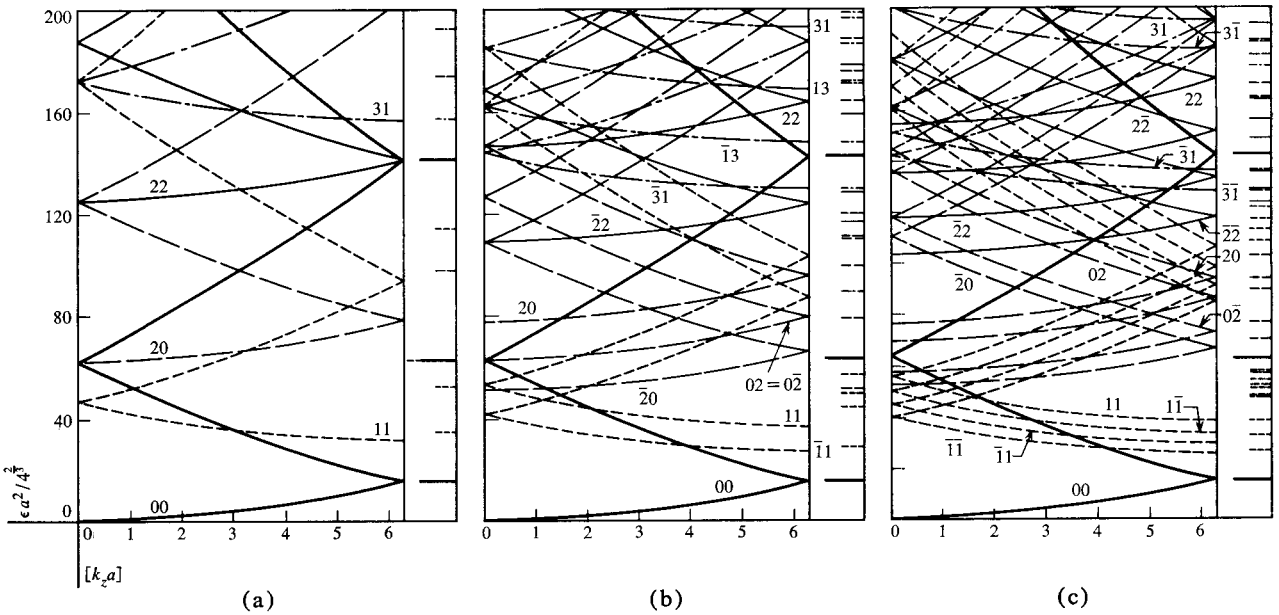

Figure 7 Free-electron energy diagrams for a beam incident with orientation (a) $\theta = \phi = 0$ (normal incidence); (b) $\theta = 6°$, $\phi = 0$; and (c) $\phi = 6°$, $\phi = 26°34'$ on a (001) surface of a face-centered cubic crystal. The ordinate unit is *rydberg-(Bohr radius)*^{2}.

Figure 8 Dependence of the energy of Bragg peaks in the 00 reflected beam on the polar angle of the incident beam for (a) $\phi = 0$ and (b) $\phi = 20°$; the surface is a (001) plane of a face-centered cubic lattice. Principal Bragg peaks are represented by solid lines and secondary peaks by dashed lines. The ordinate unit is *rydberg-(Bohr radius)*^{2}.

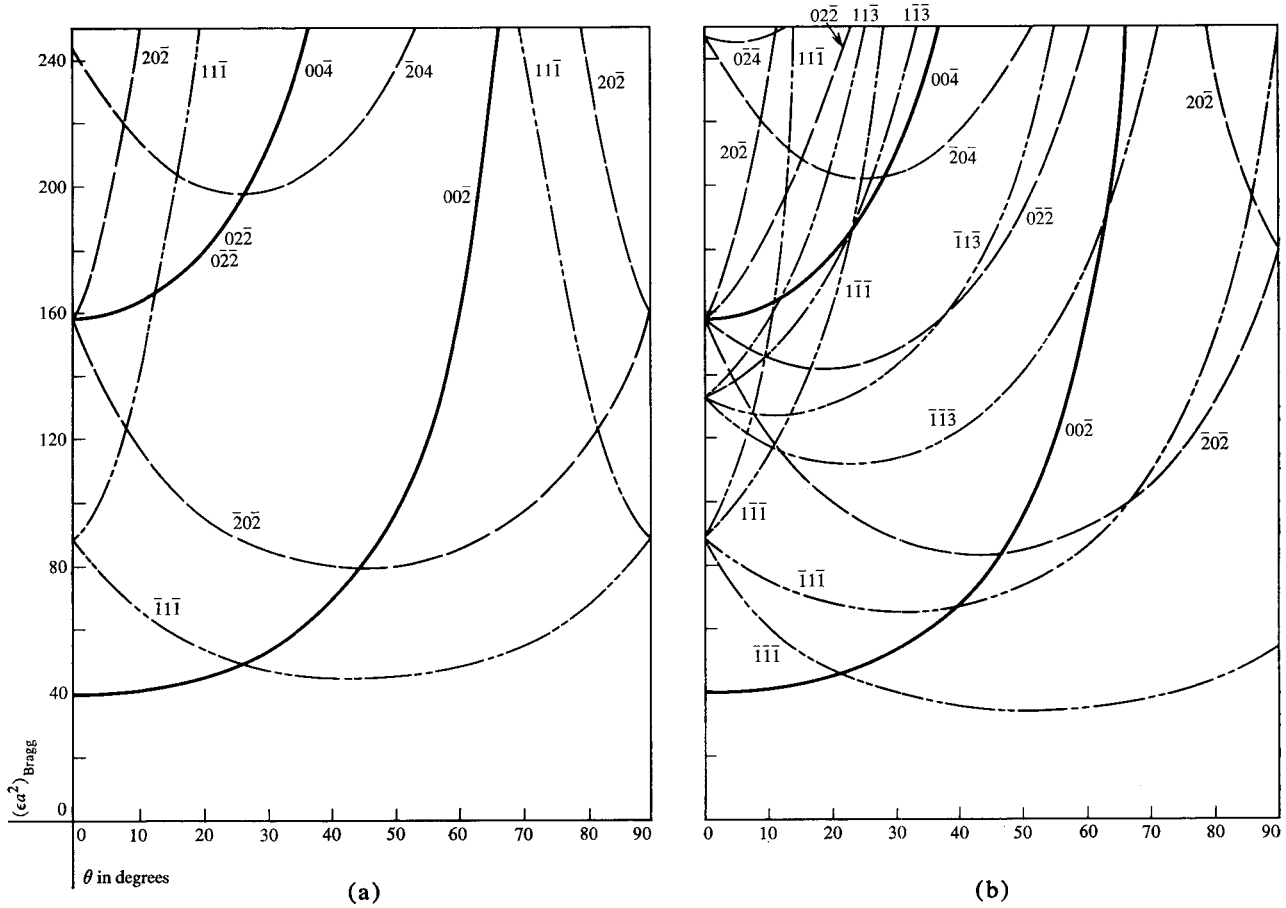

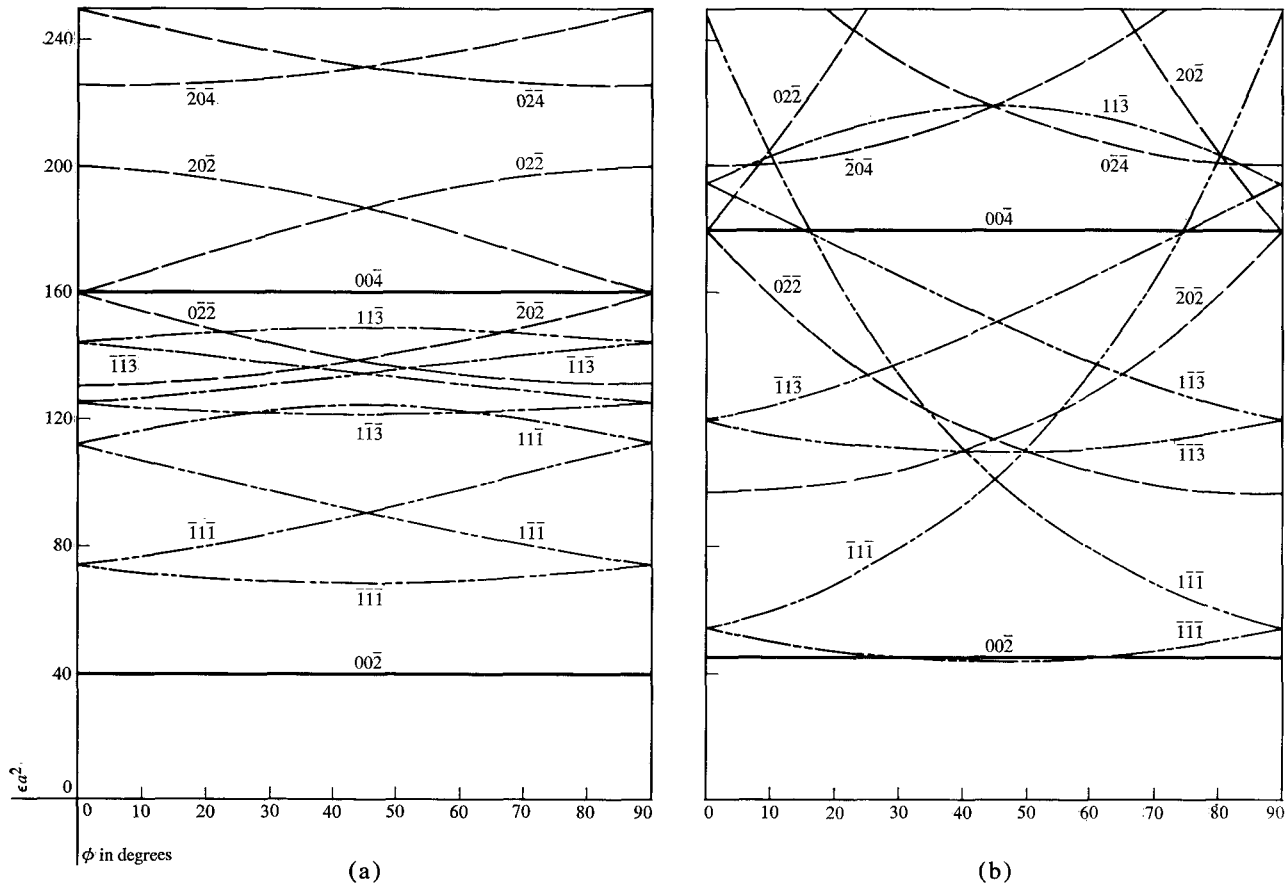

Figure 9 Dependence of the energy of Bragg peaks in the 00 reflected beam on the azimuthal angle of the incident beam for (a) $\theta = 6°$ and (b) $\theta = 20°$; the surface is a (001) plane of a face-centered cubic lattice. Principal Bragg peaks are represented by solid lines and secondary peaks by dashed lines. The ordinate unit is *rydberg-(Bohr radius)*^{2}.

wave is Bragg-reflected only for discrete members of the incident wave set that satisfy the relations (13) or (14):

$$[\mathbf{k}^i(t) + \mathbf{n}]^2 = \mathbf{k}^i(t)^2 = \epsilon(t), \tag{13}$$

which is equivalent to

$$2\mathbf{k}^i(t)\cdot\mathbf{n} = -\mathbf{n}^2. \tag{14}$$

For the case of a beam of fixed orientation as in Eq. (11), an explicit solution of Eq. (14) for the energy $\epsilon_{n_1n_2n_3}$ of the Bragg reflection denoted by integral indices n_1, n_2, n_3 is

$$\epsilon_{n_1n_2n_3} = \tfrac{1}{4}\mathbf{n}^4/[\hat{k}^i(\theta, \phi)\cdot\mathbf{n}]^2, \tag{15}$$

which generalizes Eq. (10). The energies of the complete set of Bragg reflections for the given lattice and the given orientation θ, ϕ are obtained from (15) by using all allowed values of n_1, n_2, n_3 and the known values of $\mathbf{b}_1$, $\mathbf{b}_2$, $\mathbf{b}_3$, $\hat{k}$ and their scalar products.

If the basis set $\mathbf{b}_i$ is a primitive set, i.e., if the cell volume $8\pi^3\Omega^{-1} = \mathbf{b}_1\cdot\mathbf{b}_2 \times \mathbf{b}_3$ is the maximum value (corresponding to the minimum volume Ω of the lattice cell), all reciprocal-lattice vectors $\mathbf{n}$ are obtained from all integral sets of values of n_1, n_2, n_3. However, if the $\mathbf{b}_i$ are nonprimitive and, say, $8\pi^3\Omega^{-1}$ is a fraction N^{-1} of the maximum cell volume, then n_1, n_2, n_3 take on only the fraction N^{-1} of the possible integral sets. This difference is illustrated later with cubic bases for the fcc lattice for which $N = 4$.

• *Transformations of basis and of Bragg reflection indices*

The integral indices n_i depend on the basis set and are not unique. Alternative indices n_1', n_2', n_3' for a Bragg reflection can be found by introducing a new basis $\mathbf{b}_i'$ and by expressing $\mathbf{n}$ in the new basis; i.e.,

$$\begin{aligned}\mathbf{n} &= n_1\mathbf{b}_1 + n_2\mathbf{b}_2 + n_3\mathbf{b}_3 \equiv n_i\mathbf{b}_i \\ &= n_1'\mathbf{b}_1' + n_2'\mathbf{b}_2' + n_3'\mathbf{b}_3' \equiv n_i'\mathbf{b}_i',\end{aligned} \tag{16}$$

where a repeated literal subscript implies summation over the values 1, 2 and 3. If the $\mathbf{b}_i'$ are obtained from the $\mathbf{b}_i$ by the linear transformation

$$\mathbf{b}_i' = T_{ik}\mathbf{b}_k, \tag{17}$$

the transformation on the n_j's is

$$n_k' = n_j T_{jk}^{-1}, \tag{18}$$

where the T_{jk}^{-1} are the elements of the matrix inverse to T_{jk}. If the T_{jk} are integers and if the value of the determinant $|\mathbf{T}|$ is 1, the T_{jk}^{-1} are also integers and the n_k' are integers which take on the same sets of values as the n_k.† If $|\mathbf{T}| = N^{-1}$, as in the transformation from a primitive to a nonprimitive basis set, the unit cell of the $\mathbf{b}_j'$ is one-Nth the size of the unit cell of the $\mathbf{b}_j$; the T_{jk}^{-1} and n_k' are again integers, but the n_k' do not take on as many values as do the n_k.

• *Crystal surfaces and the occurrence of beams*

In contrast with the analysis of the introductory sections, all Bragg reflections have now been described and their energies determined without reference to a surface. To complete the discussion an arbitrary surface is introduced and all Bragg reflections are assigned to the beams that characterize that surface. This assignment is carried out most easily by using the particular basis set that refers to the plane of the chosen surface. To describe that plane we need the basis vectors $\mathbf{a}_k$, $k = 1, 2, 3$, for the lattice in coordinate space, which allow any lattice translation to be described as $\mathbf{R} = l_k \mathbf{a}_k$. The $\mathbf{a}_k$ are related to the $\mathbf{b}_j$ by

$$\mathbf{a}_k \cdot \mathbf{b}_j = 2\pi \delta_{jk}; \tag{19}$$

$$\mathbf{b}_j = 2\pi \mathbf{a}_k \times \mathbf{a}_l / \Omega, \quad j, k, l \text{ in cyclic order; and} \tag{20}$$

$$\Omega \equiv \mathbf{a}_1 \cdot \mathbf{a}_2 \times \mathbf{a}_3. \tag{21}$$

Transformations to other basis sets $\mathbf{a}_k'$, corresponding to the $\mathbf{b}_j'$ and cell volume Ω', are made with the same T_{jk}^{-1} used in Eq. (18), namely

$$\mathbf{a}_k' = \mathbf{a}_j T_{jk}^{-1}, \quad \text{and} \tag{22}$$

$$\Omega' = |\mathbf{T}^{-1}|\, \Omega. \tag{23}$$

We consider a surface plane that contains the two basis vectors $\mathbf{a}_1'$ and $\mathbf{a}_2'$. This is a sufficiently general specification of a plane for all practical purposes because such planes can be chosen arbitrarily close to any desired plane. Let $\mathbf{a}_1'$, $\mathbf{a}_2'$ be primitive vectors in the two-dimensional lattice of the surface plane (the surface net) and choose an $\mathbf{a}_3'$ such that $\mathbf{a}_1'$, $\mathbf{a}_2'$, $\mathbf{a}_3'$ form a primitive set, which is always possible (see the Appendix). We can now describe the scattering of an incident plane wave beam $\exp(i\mathbf{k}^i \cdot \mathbf{r})$ by a crystal with this lattice and this surface plane. The incident beam is scattered into a set of plane waves of the form $\exp(i\mathbf{k}^s \cdot \mathbf{r})$, where the scattered wave vector $\mathbf{k}^s$ is related to the incident wave vector $\mathbf{k}^i$ by Eq. (24):

$$\mathbf{k}^s = \mathbf{k}^i + n_1' \mathbf{b}_1' + n_2' \mathbf{b}_2' + \tilde{k}_3' \mathbf{b}_3'; \tag{24}$$

here n_1' and n_2' are arbitrary integers, but $\tilde{k}_3'$ need not be an integer. Each such scattered wave has translational symmetry for displacements parallel to the surface plane; i.e., translation through a lattice vector $\mathbf{R} = l_1' \mathbf{a}_1' + l_2' \mathbf{a}_2'$ affects $\exp(i\mathbf{k}^i \cdot \mathbf{r})$ and $\exp(i\mathbf{k}^s \cdot \mathbf{r})$ the same way and leaves the phase factor $\exp(i\mathbf{k}^i \cdot \mathbf{R})$ unchanged. Note that we do not require that translational symmetry be preserved for translations *out* of the surface plane, i.e., for an $\mathbf{R}$ with a term $l_3' \mathbf{a}_3'$. This omission is appropriate because the surface discontinuity breaks the translational symmetry for displacements out of the plane.

The condition that the energy of the scattered wave be the same as that of the incident wave (the assumption of elastic scattering) determines $\tilde{k}_3'$ for given $\mathbf{k}^i$, n_1' and n_2' and for any ϵ by the relation

$$\epsilon = (\mathbf{k}^i + n_1' \mathbf{b}_1' + n_2' \mathbf{b}_2' + \tilde{k}_3' \mathbf{b}_3')^2 = (\mathbf{k}^i)^2. \tag{25}$$

For ϵ large enough, or n_1' and n_2' small enough, Eq. (25) has two real solutions for $\tilde{k}_3'$ corresponding to two scattered plane waves, each with wave vector $\mathbf{k}^s$, which have opposite components in the direction of the surface normal; thus one wave will always come out of the crystal.

For a general scattering potential with the given symmetry, a crystal with the given surface, and any $\mathbf{k}^i$, some intensity can be expected in each of the scattered beams coming out of the crystal. The beams are finite in number at any ϵ and exist and shift continuously in direction as the incident beam changes continuously. These are, in fact, the LEED "spots" for the given crystal surface and they are designated by the indices $n_1', n_2' = 0, \pm 1, \pm 2, \cdots$.‡

At certain discrete values of ϵ the corresponding $\tilde{k}_3'$ satisfies the additional condition that $\tilde{k}_3' = n_3'$; in this case $\mathbf{k}^s$ and $\mathbf{k}^i$ satisfy all the conditions for Bragg reflection. Thus the Bragg reflections assigned to or associated with the $n_1' n_2'$ beam are the $n_1' n_2' n_3'$ reflections for all integral values of n_3'. By transforming the indices n_1', n_2', n_3' back to indices n_1, n_2, n_3 in some common reference basis set $\mathbf{b}_1$, $\mathbf{b}_2$, $\mathbf{b}_3$, we can identify all Bragg reflections $n_1\, n_2\, n_3$ assigned to particular beams for the surface defined by the vectors $\mathbf{a}_1'$ and $\mathbf{a}_2'$. For the fcc lattice the natural common basis set is the cubic basis.

• *Energy diagrams for the general lattice*

As a final stage in the solution of the general problem, energy diagrams analogous to those used earlier can be introduced to describe the different beams. If Eq. (25) is solved for $\tilde{k}_3'$ for each ϵ, the total $\mathbf{b}_3'$ component of the scattered wave vector is

$$k_3^{s\prime} = k_3^{i\prime} + \tilde{k}_3' = [k_3^{s\prime}] + n_3', \quad -1 \leqq [k_3^{s\prime}] \leqq 1, \tag{26}$$

† For example, if both sets of $\mathbf{b}_j$ and $\mathbf{b}_j'$ vectors are primitive sets, the indices n_k and n_k' take on all integral values, i.e., all combinations of three integers, positive or negative.

‡ The weakened interference condition (25) for beams, as contrasted with the full interference conditions (1) and (2), corresponds to introducing "rods" in k space through the reciprocal-lattice points parallel to $\mathbf{b}_3'$ (hence perpendicular to the surface). The Ewald sphere always intersects these rods and thus indicates LEED spots at all energies in definite directions.

where n_3' is an integer† and $[k_3^s']$ is the reduced value of k_3^s'. For each pair n_1', n_2' a separate curve ϵ vs. $[k_3^s']$ can be plotted over the range -1 to 1, so that each beam is represented by a ladder-like succession of curved branches $\epsilon_{n_1'n_2'n_3'}([k_3^s'])$ for $n_3' = 0, \pm 1, \pm 2, \cdots$ which are continuous at the boundaries 1 and -1. Note that for $n_1' = n_2' = 0$, one solution of Eq. (25) is $\tilde{k}_3' = 0$; hence, $\mathbf{k}^s = \mathbf{k}^i$, the incident beam wave vector. The other solution is $\tilde{k}_3' = -2k_3^i'$; hence, $k_3^s' = -k_3^i'$, which corresponds to the specularly reflected wave, i.e., the incident wave with its component normal to the surface reversed.‡

The intersections of the branches of the 00 beam curve corresponding to the incident beam (i.e., $\epsilon_{00n_3'}([k_3^s'])$, where $[k_3^s'] = [k_3^i'])$ with the branches of the $n_1'n_2'$ beam curve corresponding to scattered waves leaving the crystal determine Bragg reflections in the beams leaving the crystal. This is a consequence of the fact that at each such intersection $\mathbf{k}^s$ and $\mathbf{k}^i$ differ by a reciprocal-lattice vector but correspond to the same value of ϵ. For the two branches involved

$$\mathbf{k}^s = (k_1^i' + n_1')\mathbf{b}_1' + (k_2^i' + n_2')\mathbf{b}_2' + \{[k_3^s'] + n_3'(n_1', n_2')\}\mathbf{b}_3'$$

on the $n_1'n_2'$ beam curve and

$$\mathbf{k}^i = k_1^i'\,\mathbf{b}_1' + k_2^i'\,\mathbf{b}_2' + \{[k_3^i'] + n_3'(0, 0)\}\mathbf{b}_3'$$

on the 00 beam curve, where $n_3'(n_1', n_2')$ denotes the value of the n_3' index on that branch of the $n_1'n_2'$ curve. Since $[k_3^s'] = [k_3^i']$ at the intersection,

$$\mathbf{k}^s - \mathbf{k}^i = n_1'\,\mathbf{b}_1' + n_2'\,\mathbf{b}_2' + n_3^{d'}\,\mathbf{b}_3', \tag{27}$$

$$n_3^{d'} = n_3'(n_1', n_2') - n_3'(0, 0) \tag{28}$$

and the intersection corresponds to the Bragg reflection $n_1'n_2'n_3^{d'}$. If $\mathbf{b}_3'$ is directed into the crystal, the incident-beam branches of the 00 beam curve have, successively, $n_3'(0, 0) = 0$ $(k_3^s' > 0)$, 1, 2, 3, $\cdots$, while the outgoing-beam branches of the $n_1'n_2'$ beam have $n_3'(n_1', n_2') = 0$ $(k_3^s' < 0)$, -1, -2, -3, $\cdots$. Therefore $n_3^{d'} \leqq 0$ from Eq. (28).

• *Application to faces of the fcc lattice*

First define the cubic basis vectors

$$\begin{aligned} \mathbf{a}_1 &= a\hat{\imath}_1, & \mathbf{b}_1 &= (2\pi/a)\hat{\imath}_1, \\ \mathbf{a}_2 &= a\hat{\imath}_2, & \mathbf{b}_2 &= (2\pi/a)\hat{\imath}_2, \\ \mathbf{a}_3 &= a\hat{\imath}_3, & \mathbf{b}_3 &= (2\pi/a)\hat{\imath}_3, \end{aligned} \tag{29}$$

where $\hat{\imath}_1$, $\hat{\imath}_2$ and $\hat{\imath}_3$ are unit vectors along the three cubic axes and a is the length of the edge of the cube. Any other basis vector can be specified by its components in the cubic basis system as a set of three numbers written in parentheses. Thus a primitive set of basis vectors for the fcc lattice can be expressed as

$$\begin{aligned} \mathbf{a}_1^p &= (0\ \tfrac{1}{2}\ \tfrac{1}{2}), & \mathbf{b}_1^p &= (\bar{1}\ 1\ 1), \\ \mathbf{a}_2^p &= (\tfrac{1}{2}\ 0\ \tfrac{1}{2}), & \mathbf{b}_2^p &= (1\ \bar{1}\ 1), \\ \mathbf{a}_3^p &= (\tfrac{1}{2}\ \tfrac{1}{2}\ 0), & \mathbf{b}_3^p &= (1\ 1\ \bar{1}), \end{aligned} \tag{30}$$

where, for example, $\mathbf{a}_1^p = (0\ \frac{1}{2}\ \frac{1}{2})$ means $\mathbf{a}_1^p = \frac{1}{2}\mathbf{a}_2 + \frac{1}{2}\mathbf{a}_3$ and $\mathbf{b}_1^p = (\bar{1}11)$ means $\mathbf{b}_1^p = -\mathbf{b}_1 + \mathbf{b}_2 + \mathbf{b}_3$, etc. From Eq. (22) we see that the components of $\mathbf{a}_k^p$ in Eq. (30) are equivalent to the elements of the transpose of the matrix $\mathbf{T}^{-1}$ which transforms cubic basis vectors into the primitive basis vectors. Since $|\mathbf{T}^{-1}| = \frac{1}{4}$ it follows that the determinant of the cubic-axis components of any primitive vector set is equal to $\frac{1}{4}$, a condition that is useful in checking the primitive sets introduced below. This value of $|\mathbf{T}^{-1}|$ corresponds to $\Omega^p = \frac{1}{4}\Omega$ and to the presence of four equivalent atoms in the cubic unit cell.

The assignment of Bragg reflections to beams for the (001), (110) and (111) surfaces of the fcc lattice requires that a primitive basis set be found for each plane with $\mathbf{a}_1'$ and $\mathbf{a}_2'$ in the plane and that the Bragg reflections in the $n_1'n_2'$ beam for that surface (which are given by integral values of n_3') be transformed to the cubic indices n_1, n_2 and n_3 by the operation inverse to that of Eq. (18), namely $n_k = n_i'T_{ik}$. Suitable sets of basis vectors for these surfaces and the corresponding transformations of indices are listed in Table 1.

The formulas given for n_1, n_2 and n_3 in Table 1 were used to determine explicitly five Bragg reflections associated with each of ten beams for the three faces of the fcc lattice (Table 2). With the convention that $\mathbf{b}_3'$ is directed into the crystal, only values of $n_3' \leqq 0$, corresponding to beams outgoing from the surface, are listed in Table 2. The n_1' and n_2' values form an arbitrary but systematic enumeration of all beams. If values of n_1', n_2', n_3' with $n_3' > 0$ are of interest, the corresponding n_1, n_2, n_3 values can be obtained by reversing all the signs in the row containing $-n_1'$, $-n_2'$, $-n_3'$.

The n_1, n_2, n_3 indices for the (001) surface show that fixed values of n_1 and n_2 still characterize each beam, as might be expected because the cubic basis vectors $\mathbf{a}_1$ and $\mathbf{a}_2$ are in the (001) plane. However, because the set $\mathbf{a}_1$, $\mathbf{a}_2$, $\mathbf{a}_3$ is not primitive, only certain index sets n_1, n_2, n_3 are allowed, namely all even or all odd integers (one-fourth of the possible sets), and the indices of the beams change; e.g., the 10 beam becomes the 11 beam while the 11 beam becomes the 20 beam.

The Bragg reflection $n_1\,n_2\,n_3$ appears in different beams for different surfaces; e.g., the 111 reflection is assigned

† The integer n_3' in Eq. (26) is not the same integer as in the discussion of Eq. (25), where n_3' corresponds to the special integral values of k_3', because an additional integer comes from replacing k_3' by its reduced value in (26). However, it is convenient to use n_3' for the integer in both cases.

‡ Note that $\mathbf{b}_3'$ is perpendicular to the surface plane because $\mathbf{a}_1'$ and $\mathbf{a}_2'$ are in that plane.

Table 1 Basis vectors and index transformations for three surfaces of the face-centered cubic lattice.

	Surface plane			*Coefficient matrix*
	(001)	(110)	(111)	
$\mathbf{a}_1'$	$(\frac{1}{2}\ \frac{1}{2}\ 0)$	$(\bar{\frac{1}{2}}\ \frac{1}{2}\ 0)$	$(0\ \frac{1}{2}\ \bar{\frac{1}{2}})$	
$\mathbf{a}_2'$	$(\frac{1}{2}\ \bar{\frac{1}{2}}\ 0)$	$(0\ 0\ 1)$	$(\frac{1}{2}\ 0\ \bar{\frac{1}{2}})$	$(\mathbf{T}^{-1})^{\mathrm{T}}$
$\mathbf{a}_3'$	$(0\ \frac{1}{2}\ \bar{\frac{1}{2}})$	$(0\ \frac{1}{2}\ \frac{1}{2})$	$(\bar{\frac{1}{2}}\ \frac{1}{2}\ 0)$	
$\mathbf{b}_1'$	$(1\ 1\ 1)$	$(\bar{2}\ 0\ 0)$	$(\bar{1}\ 1\ \bar{1})$	
$\mathbf{b}_2'$	$(1\ \bar{1}\ \bar{1})$	$(\bar{1}\ \bar{1}\ 1)$	$(1\ \bar{1}\ \bar{1})$	$\mathbf{T}$
$\mathbf{b}_3'$	$(0\ 0\ \bar{2})$	$(2\ 2\ 0)$	$(\bar{1}\ \bar{1}\ \bar{1})$	
n_1	$n_1' + n_2'$	$-2n_1' - n_2' + 2n_3'$	$-n_1' + n_2' - n_3'$	
n_2	$n_1' - n_2'$	$-n_2' + 2n_3'$	$n_1' - n_2' - n_3'$	$(\mathbf{T})^{\mathrm{T}}$
n_3	$n_1' - n_2' - 2n_3'$	n_2'	$-n_1' - n_2' - n_3'$	
n_1'	$\frac{1}{2}n_1 + \frac{1}{2}n_2$	$-\frac{1}{2}n_1 + \frac{1}{2}n_2$	$\frac{1}{2}n_2 - \frac{1}{2}n_3$	
n_2'	$\frac{1}{2}n_1 - \frac{1}{2}n_2$	n_3	$\frac{1}{2}n_1 - \frac{1}{2}n_3$	$(\mathbf{T}^{-1})^{\mathrm{T}}$
n_3'	$\frac{1}{2}n_2 - \frac{1}{2}n_3$	$\frac{1}{2}n_2 + \frac{1}{2}n_3$	$-\frac{1}{2}n_1 - \frac{1}{2}n_2$	

to the third beam for the (001) surface, to the seventh beam for the (110) surface and to the fourth beam for the (111) surface. Using the formulas for n_1', n_2', n_3' in Table 1, one could easily prepare a table enumerating n_1, n_2, n_3 systematically (as was done for n_1', n_2', n_3' in Table 2) and list for each surface the n_1', n_2', n_3' values, thus identifying the beam in which that reflection appears by the n_1', n_2' values.

For each Bragg reflection specified by its cubic indices, the corresponding energy of a beam incident at angles θ, ϕ with respect to the cubic axes is calculated using Eq. (15), which can be put in a simple form for cubic basis vectors; we find

$$\epsilon_{n_1 n_2 n_3} = \frac{\pi^2}{a^2} \frac{(n_1^2 + n_2^2 + n_3^2)^2}{(n_1 \sin\theta\cos\phi + n_2 \sin\theta\sin\phi + n_3\cos\theta)^2}. \tag{31}$$

The beam labels n_1', n_2' vary with the choice of primitive vector set, but the set of Bragg reflections or the set of n_1, n_2, n_3 values associated with a particular beam is fixed by the surface and does not change. Consequently the energy values $\epsilon_{n_1 n_2 n_3}$ of the Bragg reflections associated with one beam for a given direction of the incident beam do not depend on the choice of basis vectors.

Two characteristic properties of the Bragg reflections in a given beam should be noted particularly: (1) The vectors $\mathbf{n}$ corresponding to these reflections all have the same component parallel to the surface and differ only in the value of the component perpendicular to the surface. (Recall that in the $\mathbf{b}_1'$, $\mathbf{b}_2'$, $\mathbf{b}_3'$ basis system these vectors differ only in the value of n_3'.) The Bragg reflection points are on the rods described in the discussion of Eq. (25). (2) The Bragg reflection vectors associated with a given beam differ by multiples of l_1, l_2, l_3, the Miller indices of the surface plane. This property is obvious in the $\mathbf{a}_i'$ and $\mathbf{b}_i'$ basis sets because in these sets the Miller indices are 0, 0, 1. The property is established in the $\mathbf{a}_i$ and $\mathbf{b}_i$ basis sets from the transformation relation

$$\mathbf{b}_3' = T_{3k}\mathbf{b}_k = l_1\mathbf{b}_1 + l_2\mathbf{b}_2 + l_3\mathbf{b}_3$$

because $\mathbf{b}_3'$ is the normal vector and $n_k = n_j' T_{jk}$. Therefore, differences between the indices of any pair of Bragg reflections associated with the same beam can be expressed as

$$\Delta n_k = \Delta(n_3' T_{3k}) = (\Delta n_3') l_k$$

because n_1' and n_2' are constant for a given beam.†

† Alternatively, because Bragg reflections in the same beam differ only by a reciprocal-lattice vector along the normal, the reflections differ only by multiples of $l_1\mathbf{b}_1 + l_2\mathbf{b}_2 + l_3\mathbf{b}_3$, where l_1, l_2, l_3 are the Miller indices of the surface in the $\mathbf{b}_j$ basis. That is, $n_i^* - n_i = q l_i$, $i = 1, 2, 3$, where n_i^* and n_i are the indices of two Bragg reflections in the same beam and q is an integer. For the 00 beam all Bragg indices have the form ql_1, ql_2, ql_3.

Table 2 Beam assignments of Bragg reflections from three surfaces of the face-centered cubic lattice.

Beam	$n_1'\ n_2'\ n_3'$†	$n_1\ n_2\ n_3$ (001)	$n_1\ n_2\ n_3$ (110)	$n_1\ n_2\ n_3$ (111)
1	0 0 0	0 0 0	0 0 0	0 0 0
	0 0 $\bar{1}$	0 0 2	$\bar{2}$ $\bar{2}$ 0	1 1 1
	0 0 $\bar{2}$	0 0 4	$\bar{4}$ $\bar{4}$ 0	2 2 2
	0 0 $\bar{3}$	0 0 6	$\bar{6}$ $\bar{6}$ 0	3 3 3
	0 0 $\bar{4}$	0 0 8	$\bar{8}$ $\bar{8}$ 0	4 4 4
2	1 0 0	1 1 1	$\bar{2}$ 0 0	$\bar{1}$ 1 $\bar{1}$
	1 0 $\bar{1}$	1 1 3	$\bar{4}$ $\bar{2}$ 0	0 2 0
	1 0 $\bar{2}$	1 1 5	$\bar{6}$ $\bar{4}$ 0	1 3 1
	1 0 $\bar{3}$	1 1 7	$\bar{8}$ $\bar{6}$ 0	2 4 2
	1 0 $\bar{4}$	1 1 9	$\bar{10}$ $\bar{8}$ 0	3 5 3
3	0 1 0	1 $\bar{1}$ $\bar{1}$	$\bar{1}$ $\bar{1}$ 1	1 $\bar{1}$ $\bar{1}$
	0 1 $\bar{1}$	1 $\bar{1}$ 1	$\bar{3}$ $\bar{3}$ 1	2 0 0
	0 1 $\bar{2}$	1 $\bar{1}$ 3	$\bar{5}$ $\bar{5}$ 1	3 1 1
	0 1 $\bar{3}$	1 $\bar{1}$ 5	$\bar{7}$ $\bar{7}$ 1	4 2 2
	0 1 $\bar{4}$	1 $\bar{1}$ 7	$\bar{9}$ $\bar{9}$ 1	5 3 3
4	$\bar{1}$ 0 0	$\bar{1}$ $\bar{1}$ $\bar{1}$	2 0 0	1 $\bar{1}$ 1
	$\bar{1}$ 0 $\bar{1}$	$\bar{1}$ $\bar{1}$ 1	0 $\bar{2}$ 0	2 0 2
	$\bar{1}$ 0 $\bar{2}$	$\bar{1}$ $\bar{1}$ 3	$\bar{2}$ $\bar{4}$ 0	3 1 3
	$\bar{1}$ 0 $\bar{3}$	$\bar{1}$ $\bar{1}$ 5	$\bar{4}$ $\bar{6}$ 0	4 2 4
	$\bar{1}$ 0 $\bar{4}$	$\bar{1}$ $\bar{1}$ 7	$\bar{6}$ $\bar{8}$ 0	5 3 5
5	0 $\bar{1}$ 0	$\bar{1}$ 1 1	1 1 $\bar{1}$	$\bar{1}$ 1 1
	0 $\bar{1}$ $\bar{1}$	$\bar{1}$ 1 3	$\bar{1}$ $\bar{1}$ $\bar{1}$	0 2 2
	0 $\bar{1}$ $\bar{2}$	$\bar{1}$ 1 5	$\bar{3}$ $\bar{3}$ $\bar{1}$	1 3 3
	0 $\bar{1}$ $\bar{3}$	$\bar{1}$ 1 7	$\bar{5}$ $\bar{5}$ $\bar{1}$	2 4 4
	0 $\bar{1}$ $\bar{4}$	$\bar{1}$ 1 9	$\bar{7}$ $\bar{7}$ $\bar{1}$	3 5 5
6	1 1 0	2 0 0	$\bar{3}$ $\bar{1}$ 1	0 0 $\bar{2}$
	1 1 $\bar{1}$	2 0 2	$\bar{5}$ $\bar{3}$ 1	1 1 $\bar{1}$
	1 1 $\bar{2}$	2 0 4	$\bar{7}$ $\bar{5}$ 1	2 2 0
	1 1 $\bar{3}$	2 0 6	$\bar{9}$ $\bar{7}$ 1	3 3 1
	1 1 $\bar{4}$	2 0 8	$\bar{11}$ 9 1	4 4 2
7	$\bar{1}$ 1 0	0 $\bar{2}$ $\bar{2}$	1 $\bar{1}$ 1	2 $\bar{2}$ 0
	$\bar{1}$ 1 $\bar{1}$	0 $\bar{2}$ 0	$\bar{1}$ $\bar{3}$ 1	3 $\bar{1}$ 1
	$\bar{1}$ 1 $\bar{2}$	0 $\bar{2}$ 2	$\bar{3}$ $\bar{5}$ 1	4 0 2
	$\bar{1}$ 1 $\bar{3}$	0 $\bar{2}$ 4	$\bar{5}$ $\bar{7}$ 1	5 1 3
	$\bar{1}$ 1 $\bar{4}$	0 $\bar{2}$ 6	$\bar{7}$ $\bar{9}$ 1	6 2 4
8	$\bar{1}$ $\bar{1}$ 0	$\bar{2}$ 0 0	3 1 $\bar{1}$	0 0 2
	$\bar{1}$ $\bar{1}$ $\bar{1}$	$\bar{2}$ 0 2	1 $\bar{1}$ $\bar{1}$	1 1 3
	$\bar{1}$ $\bar{1}$ $\bar{2}$	$\bar{2}$ 0 4	0 $\bar{3}$ $\bar{1}$	2 2 4
	$\bar{1}$ $\bar{1}$ $\bar{3}$	$\bar{2}$ 0 6	$\bar{2}$ $\bar{5}$ $\bar{1}$	3 3 5
	$\bar{1}$ $\bar{1}$ $\bar{4}$	$\bar{2}$ 0 8	$\bar{5}$ $\bar{7}$ $\bar{1}$	4 4 6
9	1 $\bar{1}$ 0	0 2 2	$\bar{1}$ 1 $\bar{1}$	$\bar{2}$ 2 0
	1 $\bar{1}$ $\bar{1}$	0 2 4	$\bar{3}$ $\bar{1}$ $\bar{1}$	$\bar{1}$ 3 1
	1 $\bar{1}$ $\bar{2}$	0 2 6	$\bar{5}$ $\bar{3}$ $\bar{1}$	0 4 2
	1 $\bar{1}$ $\bar{3}$	0 2 8	$\bar{7}$ $\bar{5}$ $\bar{1}$	1 5 3
	1 $\bar{1}$ $\bar{4}$	0 2 10	$\bar{9}$ $\bar{7}$ $\bar{1}$	2 6 4
10	2 0 0	2 2 2	$\bar{4}$ 0 0	$\bar{2}$ 2 $\bar{2}$
	2 0 $\bar{1}$	2 2 4	$\bar{6}$ $\bar{2}$ 0	$\bar{1}$ 3 $\bar{1}$
	2 0 $\bar{2}$	2 2 6	$\bar{8}$ $\bar{4}$ 0	0 4 0
	2 0 $\bar{3}$	2 2 8	$\bar{10}$ $\bar{6}$ 0	1 5 1
	2 0 $\bar{4}$	2 2 10	$\bar{12}$ $\bar{8}$ 0	2 6 2

† Primed indices refer to the primitive basis vectors listed in Table 1; unprimed indices refer to the cubic basis vectors.

Appendix: Primitive basis sets in an arbitrary lattice plane

For a lattice plane specified by integral Miller indices l_1, l_2, l_3 (assumed to have no common factor) in a primitive basis set $\mathbf{a}_1^p, \mathbf{a}_2^p, \mathbf{a}_3^p$, it is useful to have a procedure for finding at least one primitive basis set $\mathbf{a}_1', \mathbf{a}_2', \mathbf{a}_3'$ in which $\mathbf{a}_1'$ and $\mathbf{a}_2'$ are in the plane. Such a basis set is a natural one for enumeration of the diffracted beams and assignment of Bragg reflections to those beams. General considerations indicate that such a primitive set always exists: An arbitrarily chosen cell (with two basis vectors in the plane) can always be examined for internal (not corner) lattice points and shorter vectors from the origin at the corner of the cell to the internal points can be chosen if

the vectors currently being considered are found not to be primitive; this process terminates in a finite number of steps with a primitive set. However, a procedure for constructing the $\mathbf{a}_i'$ can be based on a simple algebraic analysis.

The general equation of the lattice plane can be written as $\mathbf{r}\cdot\mathbf{n} = c$, where $\mathbf{r}$ is the position vector of a point in the plane, $\mathbf{n}$ is the normal to the plane and c is a constant. If $c = 0$, the plane contains the lattice point at the origin. In the basis $\mathbf{a}_i^p$ with corresponding reciprocal-lattice vectors $\mathbf{b}_i^p$ we express $\mathbf{r}$ and $\mathbf{n}$ as

$$\mathbf{r} = x_1\mathbf{a}_1^p + x_2\mathbf{a}_2^p + x_3\mathbf{a}_3^p \quad \text{and} \tag{A1}$$

$$\mathbf{n} = l_1\mathbf{b}_1^p + l_2\mathbf{b}_2^p + l_3\mathbf{b}_3^p; \tag{A2}$$

the equation of the plane is

$$l_1x_1 + l_2x_2 + l_3x_3 = 0. \tag{A3}$$

A solution of Eq. (A3) with integral values of x_1, x_2, x_3 yields a lattice vector in the given plane. A general solution of (A3) can be obtained for arbitrary integers p_1, p_2, p_3 in the form $(p_3l_2 - p_2l_3, p_1l_3 - p_3l_1, p_2l_1 - p_1l_2)$; this will be the basis vector $\mathbf{a}_1'$. For the basis vector $\mathbf{a}_2'$ we replace p_i by q_i. Let the components of $\mathbf{a}_3'$ be (T_1, T_2, T_3); values of p_i, q_i and T_i are needed that satisfy the determinantal equation

$$\begin{vmatrix} p_3l_2 - p_2l_3 & p_1l_3 - p_3l_1 & p_2l_1 - p_1l_2 \\ q_3l_2 - q_2l_3 & q_1l_3 - q_3l_1 & q_2l_1 - q_1l_2 \\ T_1 & T_2 & T_3 \end{vmatrix} = 1. \tag{A4}$$

This is the condition that makes the set $\mathbf{a}_1'$, $\mathbf{a}_2'$, $\mathbf{a}_3'$ a primitive set. Equation (A4) is equivalent to

$$(l_1T_1 + l_2T_2 + l_3T_3)\begin{vmatrix} p_1 & p_2 & p_3 \\ q_1 & q_2 & q_3 \\ l_1 & l_2 & l_3 \end{vmatrix} = 1, \tag{A5}$$

so that (A4) can be satisfied by satisfying the separate equations

$$l_1T_1 + l_2T_2 + l_3T_3 = \pm 1 \quad \text{and} \tag{A6}$$

$$p_1(q_2l_3 - q_3l_2) + p_2(q_3l_1 - q_1l_3) + p_3(q_1l_2 - q_2l_1) = \pm 1. \tag{A7}$$

The existence of solutions of Eq. (A6) for integral T_1, T_2, T_3 depends on a theorem which states that such an equation always has a solution if l_1, l_2, l_3 have no common factor (although any pair may have a common factor). This theorem follows from the basic algebraic theorem that the indeterminate equation $m_1x_1 + m_2x_2 = 1$, where m_1 and m_2 are integers with no common factor, *always* has an integral solution for x_1 and x_2.[8] Thus if l_1 and l_2 have a largest common factor f, the equation $l_1T_1 + l_2T_2 = fT_4$ has a solution for all integral T_4. For the corresponding T_1 and T_2, Eq. (A6) becomes $fT_4 + l_3T_3 = 1$, which always has a solution for T_4 and T_3 because f and l_3 have no common factor; hence (A6) is solved. Note that additional solutions of (A6) can be obtained by adding solutions of (A3), e.g., $\mathbf{a}_1'$ or $\mathbf{a}_2'$.

Similarly, Eq. (A7) always has a solution if the coefficients $q_2l_3 - q_3l_2$, $q_3l_1 - q_1l_3$ and $q_1l_2 - q_2l_1$ have no common factor. This situation can always be produced by a suitable choice of q_1, q_2, q_3. First note that q_1, q_2, q_3 can be found which satisfy $q_2l_3 - q_3l_2 = f_{23}$, $q_3l_1 - q_1l_3 = f_{31}$ and $q_1l_2 - q_2l_1 = f_{12}$, where f_{ij} is the largest common factor of l_i and l_j. However, f_{23}, f_{31} and f_{12} cannot have a common factor because this factor would then be common to l_1, l_2, l_3. Thus, defining the q's in this way, we obtain coefficients in Eq. (A7) without common factors so that (A7) can be solved for the p's. Alternatively, if $q_3l_2 - q_2l_3$, $q_1l_3 - q_3l_1$ and $q_2l_1 - q_1l_2$ have a common factor f, this factor can be canceled to give a new vector $\mathbf{a}_2'$ shorter by a factor f and now (A7) and hence (A4) have solutions for p_1, p_2, p_3. From one solution of (A7) other solutions can be obtained by adding solutions of the homogeneous form of (A7); such homogeneous solutions can be found from the coefficients of (A7) just as the solutions of (A3) were found. This procedure can be used to obtain a more convenient set of $\mathbf{a}_i'$.

To illustrate the application of Eqs. (A6) and (A7), primitive vector sets were constructed using $q_1 = q_2 = q_3 = 1$ for all planes with $l_i \leqq 4$ and with $\mathbf{a}_1'$ and $\mathbf{a}_2'$ in the plane; these sets are listed in Table 3. This procedure fails for $l_1 = l_2 = l_3 = 1$, for which case the choice $q_1 = q_3 = 0$, $q_2 = 1$ and $p_1 = 1$, $p_2 = p_3 = 0$ was made. Equivalent vector sets that keep $\mathbf{a}_1'$ and $\mathbf{a}_2'$ in the plane (l_1, l_2, l_3) can be formed by taking linear combinations of $\mathbf{a}_1'$ and $\mathbf{a}_2'$ (using integral coefficients) for which the 2×2 determinant equals one, e.g., by adding any multiple of $\mathbf{a}_2'$ to $\mathbf{a}_1'$ or any multiple of $\mathbf{a}_1'$ to $\mathbf{a}_2'$; in some cases the magnitudes of the coefficients listed in Table 3 can be reduced. Any linear combination of $\mathbf{a}_1'$ and $\mathbf{a}_2'$ could also be added to $\mathbf{a}_3'$. Table 3 applies to any primitive basis $\mathbf{a}_i^p$, $i = 1, 2, 3$, of any lattice and can be used to find a primitive vector set expressed in the $\mathbf{a}_i^p$ basis with two elements in the plane specified by the Miller indices l_i (also expressed in the $\mathbf{a}_i^p$ basis). Miller indices l_k'' in any other basis $\mathbf{a}_k''$ can be obtained by a transformation

$$l_k'' = l_jT_{jk}^{-1}, \tag{A8}$$

where T_{jk}^{-1} is the transformation from $\mathbf{a}_j^p$ to $\mathbf{a}_k''$ as in Eq. (22). Thus, in the $\mathbf{a}_k'$ basis given in the table, the Miller indices of the given plane are always 0, 0, 1.

To use Table 3 for the fcc lattice, we let the primitive basis $\mathbf{a}_i^p$ be the vectors in Eq. (30), but we specify the Miller indices of the plane in the cubic basis (29) as

Table 3 Primitive vector sets in any primitive basis with $\mathbf{a}_1'$ and $\mathbf{a}_2'$ in the (l_1, l_2, l_3) plane.

l_1 l_2 l_3	$\mathbf{a}_1'$	$\mathbf{a}_2'$	$\mathbf{a}_3'$
1 0 0	0 0 1	0 $\bar{1}$ 1	1 0 0
1 1 0	0 0 1	1 $\bar{1}$ 0	1 0 0
1 1 1	0 1 $\bar{1}$	$\bar{1}$ 0 1	1 0 0
2 1 0	0 0 1	1 $\bar{2}$ 1	0 1 0
2 1 1	$\bar{1}$ 2 0	0 $\bar{1}$ 1	0 0 1
2 2 1	$\bar{1}$ 0 2	1 $\bar{1}$ 0	0 0 1
3 1 0	0 0 1	1 $\bar{3}$ 2	0 1 0
3 1 1	$\bar{1}$ 0 3	0 $\bar{1}$ 1	0 0 1
3 2 0	$\bar{2}$ 3 0	2 $\bar{3}$ 1	1 $\bar{1}$ 0
3 2 1	0 $\bar{1}$ 2	1 $\bar{2}$ 1	0 0 1
3 2 2	$\bar{2}$ 0 3	0 $\bar{1}$ 1	1 $\bar{1}$ 0
3 3 1	0 1 $\bar{3}$	$\bar{1}$ 0 3	0 0 1
3 3 2	$\bar{2}$ 0 3	1 $\bar{1}$ 0	0 1 $\bar{1}$
4 1 0	0 0 1	1 $\bar{4}$ 3	0 1 0
4 1 1	$\bar{1}$ 0 4	0 $\bar{1}$ 1	0 0 1
4 2 1	0 $\bar{1}$ 2	1 $\bar{3}$ 2	0 0 1
4 3 0	$\bar{3}$ 4 0	3 $\bar{4}$ 1	1 $\bar{1}$ 0
4 3 1	$\bar{3}$ 4 0	2 $\bar{3}$ 1	0 0 1
4 3 2	0 $\bar{2}$ 3	1 $\bar{2}$ 1	0 1 $\bar{1}$
4 3 3	$\bar{3}$ 0 4	0 $\bar{1}$ 1	1 $\bar{1}$ 0
4 4 1	0 $\bar{1}$ 4	1 $\bar{1}$ 0	0 0 1
4 4 3	0 $\bar{3}$ 4	1 $\bar{1}$ 0	0 1 $\bar{1}$

l_1^c, l_2^c, l_3^c. Then Eq. (A8) provides the Miller indices in the primitive basis:

$$(l_1^p, l_2^p, l_3^p) = (l_1^c, l_2^c, l_3^c)\begin{pmatrix} 0 & \frac{1}{2} & \frac{1}{2} \\ \frac{1}{2} & 0 & \frac{1}{2} \\ \frac{1}{2} & \frac{1}{2} & 0 \end{pmatrix}. \tag{A9}$$

If the l_i^p obtained from Eq. (A9) are not integers, we make them integral by using a common multiplier. From Table 3 we find $\mathbf{a}_1'$, $\mathbf{a}_2'$, $\mathbf{a}_3'$ in terms of $\mathbf{a}_i^p$; i.e., the coefficients in the table are elements of $(\mathrm{T}^{-1})^{\mathrm{T}}$, which enter the transformation $\mathbf{a}_k' = \mathbf{a}_i^p T_{ik}^{-1}$. To express $\mathbf{a}_k'$ in terms of the cubic vectors $\mathbf{a}_i$ given in Eq. (29), we substitute for $\mathbf{a}_i^p$ in terms of $\mathbf{a}_i$ using the same matrix as in Eq. (A9). For example, if $l_1^c, l_2^c, l_3^c = 0, 0, 1$, respectively, Eq. (A9) yields $l_1^p, l_2^p, l_3^p = 1, 1, 0$, respectively; hence, $\mathbf{a}_1'$, $\mathbf{a}_2'$, $\mathbf{a}_3'$ in the $\mathbf{a}_i^p$ basis have the values in the second line of Table 3 and these $\mathbf{a}_i'$ can be transformed to a cubic basis as follows:

$$\begin{aligned}(\mathbf{a}_1', \mathbf{a}_2', \mathbf{a}_3') &= (\mathbf{a}_1^p, \mathbf{a}_2^p, \mathbf{a}_3^p)\begin{pmatrix} 0 & 1 & 1 \\ 0 & \bar{1} & 0 \\ 1 & 0 & 0 \end{pmatrix} \\ &= (\mathbf{a}_1, \mathbf{a}_2, \mathbf{a}_3)\begin{pmatrix} 0 & \frac{1}{2} & \frac{1}{2} \\ \frac{1}{2} & 0 & \frac{1}{2} \\ \frac{1}{2} & \frac{1}{2} & 0 \end{pmatrix}\begin{pmatrix} 0 & 1 & 1 \\ 0 & \bar{1} & 0 \\ 1 & 0 & 0 \end{pmatrix} \\ &= (\mathbf{a}_1, \mathbf{a}_2, \mathbf{a}_3)\begin{pmatrix} \frac{1}{2} & \frac{\bar{1}}{2} & 0 \\ \frac{1}{2} & \frac{1}{2} & \frac{1}{2} \\ 0 & 0 & \frac{1}{2} \end{pmatrix}.\end{aligned}$$

These vectors are listed for the (001), (011) and (111) surfaces (cubic basis) in Table 4. The $\mathbf{a}_i'$ vectors in the cubic basis are simple variants of the vectors found previously for these surfaces (Table 1) and their properties can be verified.†

† Primitive vector sets in various planes of the face-centered cubic, body-centered cubic and hexagonal close-packed lattices are given in the *Atlas* by Nicholas.[9]

Table 4 Miller indices and primitive basis vectors for three planes (with $\mathbf{a}_1'$ and $\mathbf{a}_2'$ in the given plane) expressed in cubic and primitive bases for the face-centered cubic lattice.

Plane			*Primitive basis*														
l_1^c	l_2^c	l_3^c	l_1^p	l_2^p	l_3^p	$\mathbf{a}_1'$			$\mathbf{a}_2'$			$\mathbf{a}_3'$			*Cubic basis* $\mathbf{a}_1'$			$\mathbf{a}_2'$			$\mathbf{a}_3'$		
0	0	1	1	1	0	0	0	1	1	$\bar{1}$	0	1	0	0	$\frac{1}{2}$	$\frac{1}{2}$	0	$\frac{\bar{1}}{2}$	$\frac{1}{2}$	0	0	$\frac{1}{2}$	$\frac{1}{2}$
0	1	1	2	1	1	$\bar{1}$	2	0	0	$\bar{1}$	1	0	0	1	1	$\frac{\bar{1}}{2}$	$\frac{1}{2}$	0	$\frac{1}{2}$	$\frac{\bar{1}}{2}$	$\frac{1}{2}$	$\frac{1}{2}$	0
1	1	1	1	1	1	0	1	$\bar{1}$	$\bar{1}$	0	1	1	0	0	0	$\frac{\bar{1}}{2}$	$\frac{1}{2}$	$\frac{1}{2}$	0	$\frac{\bar{1}}{2}$	0	$\frac{1}{2}$	$\frac{1}{2}$

References

1. D. S. Boudreaux and V. Heine, "Band Structure Treatment of Low Energy Electron Diffraction Intensity," *Surface Sci.* **8,** 426 (1967).
2. P. M. Marcus and D. W. Jepsen, "Accurate Calculation of Low Energy Electron Diffraction Intensities by the Propagation Matrix Method," *Phys. Rev. Letters* **20,** 925 (1968).
3. J. M. Ziman, *Principles of the Theory of Solids,* Cambridge University Press, London 1964.
4. J. C. Slater, *Symmetry and Energy Bands in Crystals* (*Quantum Theory of Molecules and Solids,* Volume 2), McGraw-Hill Book Co., Inc., New York 1965.
5. C. M. K. Watts, "Low Energy Electron Diffraction from Crystal Surfaces I. A Matrix Formulation," *J. Phys. C* (*Proc. Phys. Soc.*) **1,** 1237 (1968).
6. P. J. Jennings and E. G. McRae, "Some Comments on the Presentation of LEED Intensity Curves," LEED Theory Seminar at Cornell University, July 1968 (unpublished).
7. M. von Laue, *Roentgenstrahl-Interferenzen,* Akad. Verlagsges., Frankfurt 1960, p. 131.
8. See, for example, H. S. Hall and S. R. Knight, *Higher Algebra,* 4th Ed., MacMillan Company, New York 1891, Chap. 26.
9. J. F. Nicholas, *An Atlas of Models of Crystal Surfaces,* Gordon and Breach Science Publishers, Inc., New York 1965.

Received March 26, 1969